# Rapidly convergent iteration methods for quantum optimal control of population

Cite as: J. Chem. Phys. **108**, 1953 (1998); https://doi.org/10.1063/1.475576
Submitted: 23 May 1997 . Accepted: 24 October 1997 . Published Online: 04 June 1998

Wusheng Zhu, Jair Botina, and Herschel Rabitz

# Rapidly convergent iteration methods for quantum optimal control of population

Wusheng Zhu, Jair Botina, and Herschel Rabitz
*Department of Chemistry, Princeton University, Princeton, New Jersey 08544-1009*

(Received 23 May 1997; accepted 24 October 1997)

A family of new iteration methods is presented for designing quantum optimal controls to manipulate the transition probability. Theoretical analysis shows that these new methods exhibit quadratic and monotonic convergence. Numerical calculations verify that for these new methods, within very few steps, the optimized objective functional comes close to its convergent limit. © *1998 American Institute of Physics.* [S0021-9606(98)01205-7]

## I. INTRODUCTION

Much attention has recently been focused on optimal control of quantum systems, and extensive theoretical and numerical work has been performed.[1–5] An important case is the desire to achieve a large transition probability from a specific initial state into a final target state by means of a controlling external laser field[5] while minimizing the laser energy. For this purpose, we can construct the following objective functional, $\mathbf{J}_{fi}$, to be maximized:

$$\mathbf{J}_{fi}=|\langle\psi_i(T)|\phi_f(T)\rangle|^2-\alpha_0\times\int_0^T[\epsilon(t)]^2dt-2\,\mathrm{Re}\left[\langle\psi_i(T)|\phi_f(T)\rangle\times\int_0^T\langle\psi_f(t)|\frac{\partial}{\partial t}+i[H_0+V-\mu\epsilon(t)]|\psi_i(t)\rangle dt\right],\tag{1}$$

where $\psi_i(t)$ is the wave function driven by the optimal laser field $\epsilon(t)$. The initial wave function is $\psi_i(0)\equiv\varphi_i(0)$, and $\phi_f(T)$ is the target state specified at the final time $T$. $\alpha_0$ is a positive parameter chosen to weight the significance of the laser energy. $\psi_f(t)$ can be regarded as a Lagrange multiplier introduced to assure satisfaction of the Schrödinger equation. In the Hamiltonian, $H_0$ is the kinetic energy operator, $V$ is the potential energy, and $\mu$ is transition dipole moment. The objective functional differs from the traditional form[4,5] through the presence of the term $\langle\psi_i(T)|\phi_f(T)\rangle$ multiplying the second integral. The choice is significant since it decouples the boundary conditions of the equations for $\psi_i(t)$ and $\psi_f(t)$ as indicated in Eqs. (2) and (3). Without this factor or with other factors, the boundary conditions of Eqs. (2) and (3) would be coupled, and the algorithms presented in this paper rely on the boundary conditions being uncoupled.

Requiring $\delta\mathbf{J}_{fi}=0$ will give the equations satisfied by the wave function, Lagrange multiplier, and optimized laser field:

$$i\frac{\partial}{\partial t}\psi_i(t)=[H_0+V-\mu\epsilon(t)]\psi_i(t),\quad \psi_i(0)=\varphi_i(0),\tag{2}$$

$$i\frac{\partial}{\partial t}\psi_f(t)=[H_0+V-\mu\epsilon(t)]\psi_f(t),\quad \psi_f(T)=\phi_f(T),\tag{3}$$

$$\alpha_0\epsilon(t)=-\mathrm{Im}\langle\psi_i(t)|\psi_f(t)\rangle\langle\psi_f(t)|\mu|\psi_i(t)\rangle.\tag{4}$$

Any $\epsilon(t)$ which satisfies the above three coupled equations would be a locally optimal solution for the control problem. In the analysis below, we will make special use of the time invariant relation:

$$\langle\psi_i(T)|\phi_f(T)\rangle=\langle\psi_i(t)|\psi_f(t)\rangle\tag{5}$$

which follows from

$$\frac{d\langle\psi_i(t)|\psi_f(t)\rangle}{dt}=0\tag{6}$$

deduced using Eqs. (2) and (3). Finally substitution of Eq. (4) into Eqs. (2) and (3) gives the dynamical system to be solved:

$$i\frac{\partial}{\partial t}\psi_i(t)=(H_0+V)\psi_i(t)+\frac{\mu}{\alpha_0}\psi_i(t)\mathrm{Im}(\langle\psi_i(t)|\psi_f(t)\rangle\times\langle\psi_f(t)|\mu|\psi_i(t)\rangle),\quad \psi_i(0)=\varphi_i(0).\tag{7}$$

$$i\frac{\partial}{\partial t}\psi_f(t)=(H_0+V)\psi_f(t)+\frac{\mu}{\alpha_0}\psi_f(t)\mathrm{Im}(\langle\psi_i(t)|\psi_f(t)\rangle\times\langle\psi_f(t)|\mu|\psi_i(t)\rangle),\quad \psi_f(T)=\phi_f(T).\tag{8}$$

In order to solve the above coupled nonlinear equations, it is evident that iterative methods need to be employed. A simple iteration method based on solving the coupled Schrödinger equations by guessing an initial field to obtain $\psi_i(t)$ and $\psi_f(t)$ and using them to calculate a new field for the next iteration, etc., usually does not converge, which was tested in numerical calculations. Different iterative methods will each have their own convergence rate. In the early literature, gradient-type iteration methods combined with line searching for the control field were developed.[6–9] Later Tannor and others[4,5] suggested employing the Krotov iteration method and reported that convergence was 4 to 5 times faster than gradient-type methods. However, it is hard to analyze the general convergence behavior of the Krotov method[4] and its convergence has been observed to be as slow as gradient-

type methods if the objective functional is optimized to high accuracy[5] (e.g., to more than 80% of the converged limit).

In the following section, we will develop some novel iteration methods which incorporate feedback from the control field in an entangled fashion other than the one-step-to-next-step feedback style of the Krotov method, and the one-cycle-to-next-cycle (one cycle of iteration includes a number of steps) feedback style of gradient-type methods. In particular, these new methods will be proved to have fast quadratic monotonic convergence behavior which contributes to their high accuracy at only a few iterations. It is possible to develop a broad family of related iteration methods for solving Eqs. (7) and (8) depending on how the relation in Eq. (5) is exploited on the interval $0 \leqslant t \leqslant T$. In this paper, we shall only focus on a couple of particular choices for iteration algorithms.

## II. ITERATION ALGORITHM

Now we consider a particular iteration algorithm for solving Eqs. (7) and (8). No claim is made that the algorithm is the best choice. Indeed, later we show that there are likely even better ones in the same overall family. However, the analysis below is generic and may be extended to the other members of the family. The iteration procedure is specified as follows:

Step 1:

$$i\frac{\partial}{\partial t}\psi_f^{(0)}(t)=(H_0+V)\psi_f^{(0)}(t)-\mu\overline{\epsilon(t)}\psi_f^{(0)}(t), \tag{9}$$

$$i\frac{\partial}{\partial t}\psi_i^{(1)}(t)=(H_0+V)\psi_i^{(1)}(t)+\frac{\mu}{\alpha_0}\psi_i^{(1)}(t) \times \mathrm{Im}(\langle\psi_i^{(1)}(t)|\psi_f^{(0)}(t)\rangle\langle\psi_f^{(0)}(t)|\mu|\psi_i^{(1)}(t)\rangle). \tag{10}$$

Step 2:

$$i\frac{\partial}{\partial t}\psi_f^{(1)}(t)=(H_0+V)\psi_f^{(1)}(t)+\frac{\mu}{\alpha_0}\psi_f^{(1)}(t) \times \mathrm{Im}(\langle\psi_i^{(1)}(t)|\psi_f^{(1)}(t)\rangle\langle\psi_f^{(1)}(t)|\mu|\psi_i^{(1)}(t)\rangle), \tag{11}$$

$$i\frac{\partial}{\partial t}\psi_i^{(2)}(t)=(H_0+V)\psi_i^{(2)}(t)+\frac{\mu}{\alpha_0}\psi_i^{(2)}(t) \times \mathrm{Im}(\langle\psi_i^{(2)}(t)|\psi_f^{(1)}(t)\rangle\langle\psi_f^{(1)}(t)|\mu|\psi_i^{(2)}(t)\rangle), \tag{12}$$

$$\vdots$$

The algorithm is defined by the choice for interpreting $\langle\psi_i(t)|\psi_f(t)\rangle$ through the flexibility inherent in the time invariance of Eq. (6). The corresponding control field at each iteration step can be written as

$$\overline{\epsilon(t)}=0(\text{or another chosen function}),$$

$$\alpha_0\epsilon^{(0)}(t)=-\mathrm{Im}(\langle\psi_i^{(1)}(t)|\psi_f^{(0)}(t)\rangle\langle\psi_f^{(0)}(t)|\mu|\psi_i^{(1)}(t)\rangle), \tag{13}$$

$$\alpha_0\epsilon^{(1)}(t)=-\mathrm{Im}(\langle\psi_i^{(1)}(t)|\psi_f^{(1)}(t)\rangle\langle\psi_f^{(1)}(t)|\mu|\psi_i^{(1)}(t)\rangle), \tag{14}$$

$$\alpha_0\epsilon^{(2)}(t)=-\mathrm{Im}(\langle\psi_i^{(2)}(t)|\psi_f^{(1)}(t)\rangle\langle\psi_f^{(1)}(t)|\mu|\psi_i^{(2)}(t)\rangle), \tag{15}$$

$$\vdots$$

Before discussing convergence behavior, there are some interesting features worth high-lighting.

First, if we choose $\overline{\epsilon(t)}=0$ as the input to Eqs. (9)–(12), in some cases, the calculation may remain locked in the trivial solution to the optimal control problem. For example, in the optimal control problem of steering the system from one eigenstate to another, the initial wave packet $\varphi_i$ is orthogonal to the target wave packet $\phi_f$. The trivial solution satisfying Eqs. (7) and (8) consistent with $\overline{\epsilon(t)}=0$ is

$$\epsilon(t)=0,$$

$$\psi_i(t)=\exp[-i(H_0+V)t]\varphi_i(0)\equiv\varphi_i(t),$$

$$\psi_f(t)=\exp[-i(H_0+V)(t-T)]\phi_f(T)\equiv\phi_f(t). \tag{16}$$

This situation is undesirable as no transition will result. Fortunately, numerical tests show that this trivial solution corresponds to an unstable extremum point, although it satisfies the variational principle. The numerical iteration will quickly leave that point and converge to another stable point corresponding to a nontrivial control solution.

Second, we may also show that it is not possible to exactly control the target state, $\psi_i(T)\rightarrow\phi_f(T)$ (up to an arbitrary phase),

$$|\langle\psi_i(T)\phi_f(T)\rangle|^2=|\langle\psi_i(t)|\psi_f(t)\rangle|^2\neq 1. \tag{17}$$

In order to prove this statement, we expand the wave function in a complete basis formed by all products:

$$\psi_i(t)=\sum_{\{\mathbf{f}\}=\{f,f',f'',\ldots\}}\langle\psi_{\{\mathbf{f}\}}(t)|\psi_i(t)\rangle\psi_{\{\mathbf{f}\}}(t). \tag{18}$$

If we assume that the product goes exclusively to the $f$ channel, we have

$$\psi_i(t)=\langle\psi_f(t)|\psi_i(t)\rangle\psi_f(t) \tag{19}$$

and then the optimized electric field would be

$$\begin{aligned}\alpha_0\epsilon(t)&=-\mathrm{Im}(\langle\psi_i(t)|\psi_f(t)\rangle\langle\psi_f(t)|\mu|\psi_i(t)\rangle)\\&=-\mathrm{Im}(\langle\psi_f(t)|\psi_i(t)\rangle\langle\psi_i(t)|\psi_f(t)\rangle\langle\psi_f(t)|\mu|\psi_f(t)\rangle)\\&=-\mathrm{Im}(\langle\psi_f(t)|\mu|\psi_f(t)\rangle)|\langle\psi_f(t)|\psi_i(t)\rangle|^2\\&=0,\end{aligned} \tag{20}$$

where we used the fact that the expectation value of the dipole operator is always real. This circumstance could only happen in the trivial case of starting out in the target state. We may also understand this behavior in terms of $\alpha_0>0$ generally preventing exact achievement of the target state even if the system is controllable.

## III. CONVERGENCE BEHAVIOR OF THE ITERATION ALGORITHM

After the first iteration step, the field in Eq. (13) may be rewritten with the aid of Eqs. (9) and (10) as

$$\begin{aligned}\alpha_0\epsilon^{(0)}(t) &= -\mathrm{Im}(\langle\psi_i^{(1)}(t)|\psi_f^{(0)}(t)\rangle\langle\psi_f^0(t)|\mu|\psi_i^{(1)}(t)\rangle)\\ &= -\mathrm{Im}\left(\frac{i}{\overline{\epsilon(t)}-\epsilon^{(0)}(t)}\frac{\partial\langle\psi_f^{(0)}(t)|\psi_i^{(1)}(t)\rangle}{\partial t}\right.\\ &\quad\left.\times\langle\psi_i^{(1)}(t)|\psi_f^{(0)}(t)\rangle\right)\\ &= \frac{1}{2[\epsilon^{(0)}(t)-\overline{\epsilon(t)}]}\frac{\partial|\langle\psi_f^{(0)}(t)|\psi_i^{(1)}(t)\rangle|^2}{\partial t},\end{aligned}\tag{21}$$

or equivalently

$$\frac{\partial|\langle\psi_f^{(0)}(t)|\psi_i^{(1)}(t)\rangle|^2}{\partial t}=2\alpha_0\epsilon^{(0)}(t)[\epsilon^{(0)}(t)-\overline{\epsilon(t)}].\tag{22}$$

After integration over $t$ from 0 to $T$, we obtain

$$\begin{aligned}|\langle\phi_f(T)|\psi_i^{(1)}(T)\rangle|^2 &= |\langle\psi_f^{(0)}(0)|\varphi_i(0)\rangle|^2+2\alpha_0\int_0^T\epsilon^{(0)}(t)\\ &\quad\times[\epsilon^{(0)}(t)-\overline{\epsilon(t)}]dt,\end{aligned}\tag{23}$$

which may be identified as the optimally achieved probability after the first iteration step. We can then determine the objective functional in Eq. (1) after one iteration step:

$$\begin{aligned}\mathbf{J}_{fi}^{(0)} &= |\langle\psi_f^{(0)}(0)|\varphi_i(0)\rangle|^2+2\alpha_0\int_0^T\epsilon^{(0)}(t)\\ &\quad\times[\epsilon^{(0)}(t)-\overline{\epsilon(t)}]dt-\alpha_0\int_0^T[\epsilon^{(0)}(t)]^2dt.\end{aligned}\tag{24}$$

Similarly, at the second iteration step in Eq. (14), we have

$$\begin{aligned}\alpha_0\epsilon^{(1)}(t) &= -\mathrm{Im}(\langle\psi_i^{(1)}(t)|\psi_f^{(1)}(t)\rangle\langle\psi_f^{(1)}(t)|\mu|\psi_i^{(1)}(t)\rangle)\\ &= -\mathrm{Im}\left(\frac{i}{\epsilon^{(1)}(t)-\epsilon^{(0)}(t)}\frac{\partial\langle\psi_f^{(1)}(t)|\psi_i^{(1)}(t)\rangle}{\partial t}\right.\\ &\quad\left.\times\langle\psi_i^{(1)}(t)|\psi_f^{(1)}(t)\rangle\right)\\ &= \frac{1}{2[\epsilon^{(0)}(t)-\epsilon^{(1)}(t)]}\frac{\partial|\langle\psi_f^{(1)}(t)|\psi_i^{(1)}(t)\rangle|^2}{\partial t}\end{aligned}\tag{25}$$

which is equivalent to

$$\frac{\partial|\langle\psi_f^{(1)}(t)|\psi_i^{(1)}(t)\rangle|^2}{\partial t}=2\alpha_0\epsilon^{(1)}(t)[\epsilon^{(0)}(t)-\epsilon^{(1)}(t)].\tag{26}$$

Integration over $t$ from 0 to $T$ yields

$$\begin{aligned}|\langle\psi_f^{(1)}(0)|\varphi_i(0)\rangle|^2 &= |\langle\phi_f(T)|\psi_i^{(1)}(T)\rangle|^2+2\alpha_0\int_0^T\epsilon^{(1)}(t)\\ &\quad\times[\epsilon^{(1)}(t)-\epsilon^{(0)}(t)]dt.\end{aligned}\tag{27}$$

Inserting Eq. (23) produces

$$\begin{aligned}|\langle\psi_f^{(1)}(0)|\varphi_i(0)\rangle|^2 &= |\langle\psi_f^{(0)}(0)|\varphi_i(0)\rangle|^2+2\alpha_0\int_0^T\epsilon^{(0)}(t)\\ &\quad\times[\epsilon^{(0)}(t)-\overline{\epsilon(t)}]dt+2\alpha_0\\ &\quad\times\int_0^T\epsilon^{(1)}(t)[\epsilon^{(1)}(t)-\epsilon^{(0)}(t)]dt.\end{aligned}\tag{28}$$

After finishing the second iteration step and following a similar procedure used to derive Eq. (23), we will obtain

$$\begin{aligned}|\langle\phi_f(T)|\psi_i^{(2)}(T)\rangle|^2 &= |\langle\psi_f^{(1)}(0)|\varphi_i(0)\rangle|^2+2\alpha_0\int_0^T\epsilon^{(2)}(t)\\ &\quad\times[\epsilon^{(2)}(t)-\epsilon^{(1)}(t)]dt.\end{aligned}\tag{29}$$

Inserting the result of Eq. (28), we have the following expression for the optimized transition probability

$$\begin{aligned}|\langle\phi_f(T)|\psi_i^{(2)}(T)\rangle|^2 &= |\langle\psi_f^{(0)}(0)|\varphi_i(0)\rangle|^2+2\alpha_0\int_0^T\epsilon^{(0)}(t)\\ &\quad\times[\epsilon^{(0)}(t)-\overline{\epsilon(t)}]dt+2\alpha_0\int_0^T\epsilon^{(1)}(t)\\ &\quad\times[\epsilon^{(1)}(t)-\epsilon^{(0)}(t)]dt\\ &\quad+2\alpha_0\int_0^T\epsilon^{(2)}(t)[\epsilon^{(2)}(t)-\epsilon^{(1)}(t)]dt\end{aligned}\tag{30}$$

and the objective functional

$$\begin{aligned}\mathbf{J}_{fi}^{(1)} &= |\langle\psi_f^{(0)}(0)|\varphi_i(0)\rangle|^2+2\alpha_0\int_0^T\epsilon^{(0)}(t)[\epsilon^{(0)}(t)-\overline{\epsilon(t)}]dt\\ &\quad-\alpha_0\int_0^T[\epsilon^{(2)}(t)]^2dt+2\alpha_0\int_0^T\epsilon^{(1)}(t)[\epsilon^{(1)}(t)-\epsilon^{(0)}(t)]\\ &\quad\times dt+2\alpha_0\int_0^T\epsilon^{(2)}(t)[\epsilon^{(2)}(t)-\epsilon^{(1)}(t)]dt.\end{aligned}\tag{31}$$

Given the above analysis, we may generalize these results and address the convergence rate of the iteration algorithm. Defining $\delta\epsilon_{k+1,k}\equiv\epsilon^{(k+1)}(t)-\epsilon^{(k)}(t)$, $k=0,1,2,...$ and $\delta\mathbf{J}_{10}\equiv\mathbf{J}_{fi}^{(1)}-\mathbf{J}_{fi}^{(0)}$, we will get the following expression for the deviation of the objective functional:

$$\begin{aligned}\delta\mathbf{J}_{10} &= \alpha_0\int_0^T[\epsilon^{(0)}(t)]^2dt-\alpha_0\int_0^T[\epsilon^{(2)}(t)]^2dt+2\alpha_0\\ &\quad\times\int_0^T\epsilon^{(1)}(t)[\epsilon^{(1)}(t)-\epsilon^{(0)}(t)]dt+2\alpha_0\int_0^T\epsilon^{(2)}(t)\\ &\quad\times[\epsilon^{(2)}(t)-\epsilon^{(1)}(t)]dt\\ &= \alpha_0\int_0^T(|\delta\epsilon_{10}|^2+|\delta\epsilon_{21}|^2)dt.\end{aligned}\tag{32}$$

The $(N+1)$th iteration step optimized transition probability can be expressed as

$$\begin{aligned}|P_{fi}^{(N)}|^2 &= |\langle \phi_f(T)|\psi_i^{(N+1)}(T)\rangle|^2 \\ &= |\langle \psi_f^{(0)}(0)|\varphi_i(0)\rangle|^2 \\ &\quad + 2\alpha_0 \int_0^T \epsilon^{(0)}(t)[\epsilon^{(0)}(t) - \overline{\epsilon(t)}]dt \\ &\quad + 2\alpha_0 \int_0^T \sum_{k=0}^{2N-1} \epsilon^{(k+1)}(t)[\epsilon^{(k+1)}(t) - \epsilon^{(k)}(t)]dt\end{aligned} \tag{33}$$

and the corresponding optimized objective functional is

$$\begin{aligned}\mathbf{J}_{fi}^{(N)} &= |\langle \psi_f^{(0)}(0)|\varphi_i(0)\rangle|^2 + 2\alpha_0 \int_0^T \epsilon^{(0)}(t) \\ &\quad \times [\epsilon^{(0)}(t) - \overline{\epsilon(t)}]dt - \alpha_0 \int_0^T [\epsilon^{(2N)}(t)]^2 dt \\ &\quad + 2\alpha_0 \int_0^T \sum_{k=0}^{2N-1} \epsilon^{(k+1)}(t)[\epsilon^{(k+1)}(t) - \epsilon^{(k)}(t)]dt.\end{aligned} \tag{34}$$

The total difference between the first iteration step and the $(N+1)$th iteration step optimized objective functionals is

$$\delta \mathbf{J}_{N0} \equiv \mathbf{J}_{fi}^{(N)} - \mathbf{J}_{fi}^{(0)} = \alpha_0 \int_0^T \sum_{k=0}^{2N-1} |\delta \epsilon_{k+1,k}|^2 dt. \tag{35}$$

Examination of Eq. (35) shows that the algorithm has bounded variational character with the following properties: (i) The iteration sequence converges monotonically and quadratically in terms of the neighboring field deviations. (ii) Since the optimal control problem is designed for maximizing the objective functional, a larger deviation of the field between neighboring steps will lead to faster convergence of the objective functional. The initial trial field $\overline{\epsilon(t)}$ will typically be far from the exact solution, and thus we expect that the first few iteration steps will give the major contribution to the rapid convergence of the cost functional. However, the same logic suggests that the fractional rate of convergence will slow down after the initial high gain.

Finally for completeness, the symmetric analog of the algorithm is presented below by starting with $\psi_i^{(0)}(t)$ instead of $\psi_f^{(0)}(t)$:

Step 1:

$$i\frac{\partial}{\partial t}\psi_i^{(0)}(t) = (H_0+V)\psi_i^{(0)}(t) - \mu\overline{\epsilon(t)}\psi_i^{(0)}(t), \tag{36}$$

$$\begin{aligned}i\frac{\partial}{\partial t}\psi_f^{(1)}(t) &= (H_0+V)\psi_f^{(1)}(t) + \frac{\mu}{\alpha_0}\psi_f^{(1)}(t) \\ &\quad \times \mathrm{Im}(\langle \psi_i^{(0)}(t)|\psi_f^{(1)}(t)\rangle\langle \psi_f^{(1)}(t)|\mu|\psi_i^{(0)}(t)\rangle).\end{aligned} \tag{37}$$

Step 2:

$$\begin{aligned}i\frac{\partial}{\partial t}\psi_i^{(1)}(t) &= (H_0+V)\psi_i^{(1)}(t) + \frac{\mu}{\alpha_0}\psi_i^{(1)}(t) \\ &\quad \times \mathrm{Im}(\langle \psi_i^{(1)}(t)|\psi_f^{(1)}(t)\rangle\langle \psi_f^{(1)}(t)|\mu|\psi_i^{(1)}(t)\rangle),\end{aligned} \tag{38}$$

$$\begin{aligned}i\frac{\partial}{\partial t}\psi_f^{(2)}(t) &= (H_0+V)\psi_f^{(2)}(t) + \frac{\mu}{\alpha_0}\psi_f^{(2)}(t) \\ &\quad \times \mathrm{Im}(\langle \psi_i^{(1)}(t)|\psi_f^{(2)}(t)\rangle\langle \psi_f^{(2)}(t)|\mu|\psi_i^{(1)}(t)\rangle, \\ &\quad \vdots\end{aligned} \tag{39}$$

The corresponding control field at each iteration step can be written as

$$\overline{\epsilon(t)} = 0 \quad \text{(or another chosen function)},$$

$$\alpha_0\epsilon^{(0)}(t) = -\mathrm{Im}(\langle \psi_i^{(0)}(t)|\psi_f^{(1)}(t)\rangle\langle \psi_f^{(1)}(t)|\mu|\psi_i^0(t)\rangle), \tag{40}$$

$$\alpha_0\epsilon^{(1)}(t) = -\mathrm{Im}(\langle \psi_i^{(1)}(t)|\psi_f^{(1)}(t)\rangle\langle \psi_f^{(1)}(t)|\mu|\psi_i^{(1)}(t)\rangle), \tag{41}$$

$$\alpha_0\epsilon^{(2)}(t) = -\mathrm{Im}(\langle \psi_i^{(1)}(t)|\psi_f^{(2)}(t)\rangle\langle \psi_f^{(2)}(t)|\mu|\psi_i^{(1)}(t)\rangle), \tag{42}$$

$$\vdots$$

A detailed analysis shows the same convergence behavior for this variant of the algorithm. A family of related algorithms may also be generated possibly exhibiting even faster overall convergence behavior. One such algorithm is presented in the Appendix.

## IV. DISCRETE IMPLEMENTATION OF THE ALGORITHM

In practice, we must choose an appropriate discrete propagation method to evaluate the algorithm. A simple approach would adopt the first-order split-operator method,

Step 1:

$$\begin{aligned}&\psi_f^{(0)}(t_0-\Delta t) = e^{iH_0\Delta t}e^{i[V-\mu\overline{\epsilon}(t_0)]\Delta t}\psi_f^{(0)}(t_0), \\ &\psi_f^{(0)}(T) = \phi_f(T), \\ &\psi_i^{(1)}(t_0+\Delta t) = e^{-iH_0\Delta t}e^{-i[V-\mu\epsilon^{(0)}(t_0)]\Delta t}\psi_i^{(1)}(t_0), \\ &\epsilon^{(0)}(t_0) = -\frac{1}{\alpha_0}\mathrm{Im}(\langle \psi_i^{(1)}(t_0)|\psi_f^{(0)}(t_0)\rangle \\ &\qquad \times \langle \psi_f^{(0)}(t_0)|\mu|\psi_i^{(1)}(t_0)\rangle) \\ &\qquad \times \psi_i^{(0)}(0) = \varphi_i(0),\end{aligned} \tag{43, 44}$$

Step 2:

$$\begin{aligned}&\psi_f^{(1)}(t_0-\Delta t) = e^{iH_0\Delta t}e^{i[V-\mu\epsilon^{(1)}(t_0)]\Delta t}\psi_f^{(1)}(t_0), \\ &\epsilon^{(1)}(t_0) = -\frac{1}{\alpha_0}\mathrm{Im}(\langle \psi_i^{(1)}(t_0)|\psi_f^{(1)}(t_0)\rangle \\ &\qquad \times \langle \psi_f^{(1)}(t_0)|\mu|\psi_i^{(1)}(t_0)\rangle) \\ &\qquad \times \psi_f^{(1)}(T) = \phi_f(T),\end{aligned} \tag{45}$$

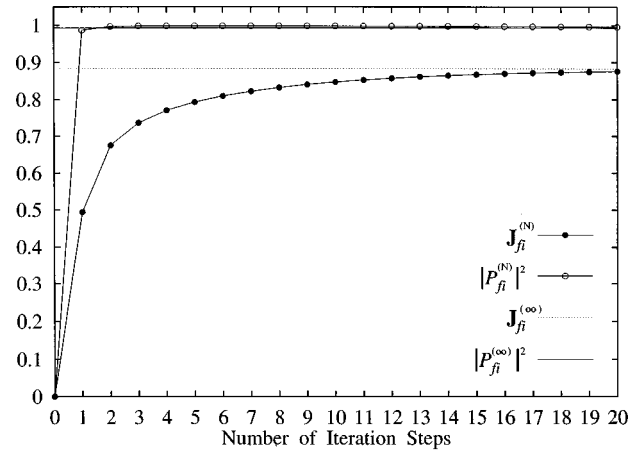


FIG. 1. Optimized objective functional $\mathbf{J}_{fi}^{(N)}$ and transition probability $|P_{fi}^{(N)}|^2$ for the transition of $v=0\rightarrow v=1$. Rapid monotonic convergence is found.

$$\psi_i^{(2)}(t_0+\Delta t)=e^{-H_0\Delta t}e^{-i[V-\mu\epsilon^{(2)}(t_0)]\Delta t}\psi_i^{(2)}(t_0),$$

$$\epsilon^{(2)}(t_0)=-\frac{1}{\alpha_0}\,\mathrm{Im}(\langle\psi_i^{(2)}(t_0)|\psi_f^{(1)}(t_0)\rangle \times\langle\psi_f^{(1)}(t_0)|\mu|\psi_i^{(2)}(t_0)\rangle),$$

$$\psi_i^{(2)}(0)=\varphi_i(0),$$

$$\vdots \tag{46}$$

The first-order method has some similar features to the Krotov method.[4,5] A more efficient discrete propagation method may be generated based on the second-order split-operator technique,

Step 1:

$$\psi_f^{(0)}(t_0-\Delta t)=e^{iH_0\Delta t/2}e^{i[V-\mu\overline{\epsilon(}t_0-\Delta t/2)]\Delta t} \times e^{iH_0\Delta t/2}\psi_f^{(0)}(t_0),$$

$$\psi_f^{(0)}(T)=\phi_f(T), \tag{47}$$

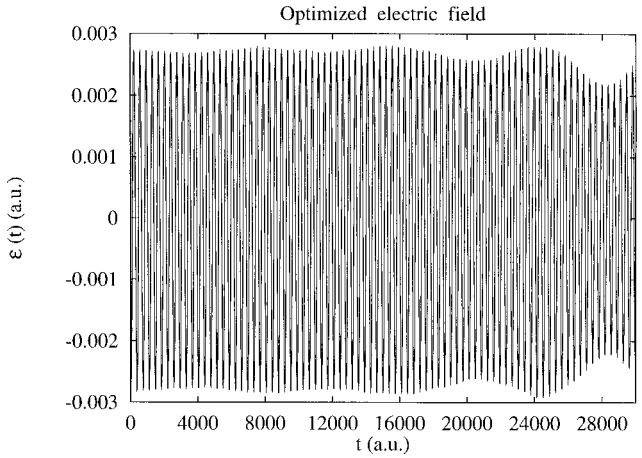


FIG. 2. Optimized electric field time dependence for the transition of $v=0\rightarrow v=1$. It is almost a pure cosine function.

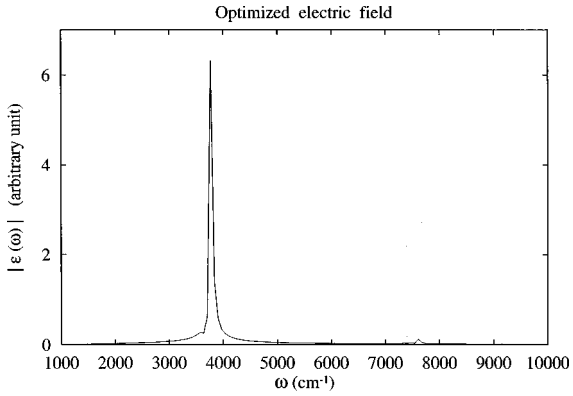


FIG. 3. Power spectrum of the field in Fig. 2. The dominant frequency matches the $0\rightarrow 1$ resonant condition.

$$\psi_i^{(1)}(t_0+\Delta t)=e^{-iH_0\Delta t/2}e^{-i[V-\mu\epsilon^{(0)}(t_0+\Delta t/2)]\Delta t} \times e^{-iH_0\Delta t/2}\psi_i^{(1)}(t_0),$$

$$\epsilon^{(0)}(t_0+\Delta t/2)=-\frac{1}{\alpha_0}\,\mathrm{Im}\Big(\langle\psi_i^{(1)}(t_0)|\psi_f^{(0)}(t_0)\rangle \times\langle\psi_f^{(0)}(t_0)|\mu-\frac{i\Delta t}{2}[\mu,H_0]|\psi_i^{(1)}(t_0)\rangle\Big),$$

$$\psi_i^{(1)}(0)=\varphi_i(0), \tag{48}$$

Step 2:

$$\psi_f^{(1)}(t_0-\Delta t)=e^{iH_0\Delta t/2}e^{i[V-\mu\epsilon^{(1)}(t_0-\Delta t/2)]\Delta t} \times e^{iH_0\Delta t/2}\psi_f^{(1)}(t_0),$$

$$\epsilon^{(1)}(t_0-\Delta t/2)=-\frac{1}{\alpha_0}\,\mathrm{Im}\Big(\langle\psi_i^{(1)}(t_0)|\psi_f^{(1)}(t_0)\rangle \times\langle\psi_f^{(1)}(t_0)|\mu+\frac{i\Delta t}{2}[\mu,H_0]|\psi_i^{(1)}(t_0)\rangle\Big)$$

$$\psi_f^{(1)}(T)=\phi_f(T), \tag{49}$$

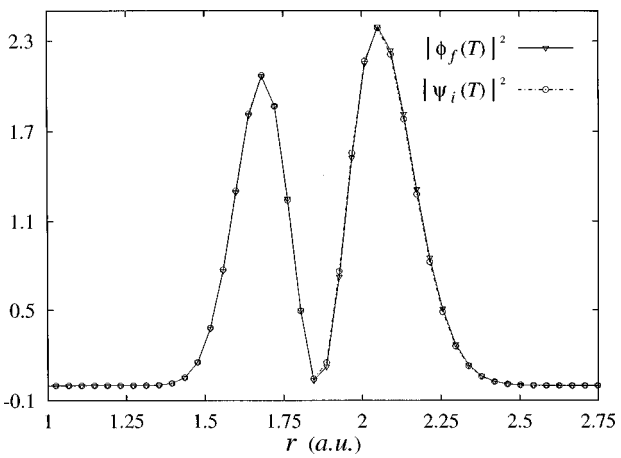


FIG. 4. Specified final wave function $|\phi_f(T)|^2$ for $v=1$ and the optimized wave function from $v=0$ at the final time $|\psi_i(T)|^2$.

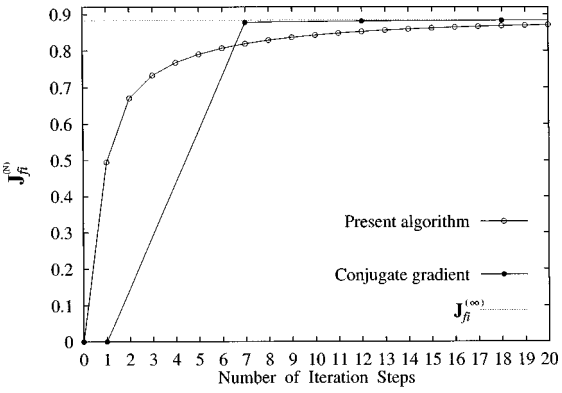


FIG. 5. Comparison of the convergence behavior of the optimized objective functional $\mathbf{J}_{fi}^{(N)}$ calculated by the new algorithm and the conjugate gradient method. Each step of the conjugate gradient method costs the equivalent of several steps of the new algorithm, as indicated by the spacing of the points. The convergence of the conjugate gradient method is sensitive to the initial guess (the figure shows the best case that was found) while the new algorithm was observed to be very insensitive.

$$\psi_i^{(2)}(t_0+\Delta t)=e^{-iH_0\Delta t/2}e^{-i[V-\mu\epsilon^{(2)}(t_0+\Delta t/2)]\Delta t}e^{-iH_0\Delta t/2}\times\psi_i^{(2)}(t_0),$$

$$\epsilon^{(2)}(t_0+\Delta t/2)=-\frac{1}{\alpha_0}\,\mathrm{Im}\left(\langle\psi_i^{(2)}(t_0)|\psi_f^{(1)}(t_0)\rangle\times\langle\psi_f^{(1)}(t_0)|\mu-\frac{i\Delta t}{2}[\mu,H_0]|\psi_i^{(2)}(t_0)\rangle\right)$$

$$\psi_i^{(2)}(0)=\varphi_i(0),$$

$$\vdots \tag{50}$$

where we have considered the Taylor expansion of the laser field up to the first order:

$$\epsilon(t+\delta t)=\epsilon(t)+\frac{\partial\epsilon(t)}{\partial t}\,\delta t. \tag{51}$$

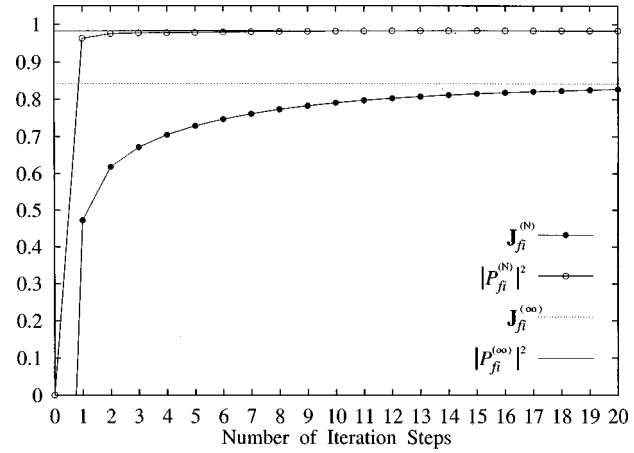


FIG. 6. Optimized objective functional $\mathbf{J}_{fi}^{(N)}$ and transition probability $|P_{fi}^{(N)}|^2$ for the transition of $v=4\rightarrow v=5$. Rapid monotonic convergence is found.

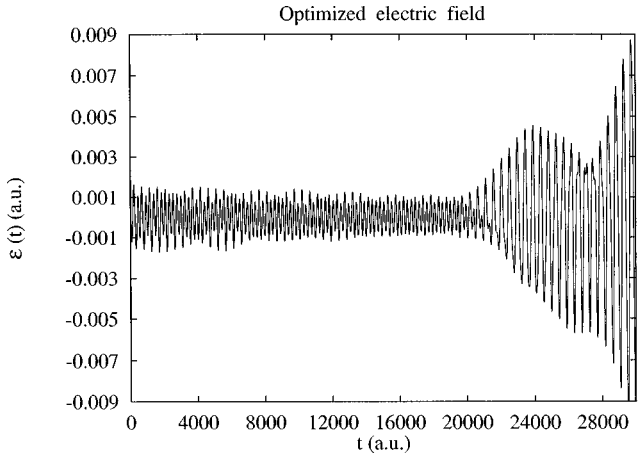


FIG. 7. Optimized electric field time dependence for the transition of $v=4\rightarrow v=5$. Two or more frequencies are interfering.

Roughly, in order to reach the same accuracy, a time step in the second-order scheme of Eqs. (47)–(50) can be ten times larger than that in the first-order scheme of Eqs. (43)–(46), while each iteration step in the second-order scheme will cost about twice as much as that in the first-order scheme. Thus we anticipate that the efficiency of the second-order scheme will be about five times higher than that of the first-order scheme. This behavior was verified in numerical tests and below only the results of the second-order scheme will be reported.

## V. NUMERICAL TESTS OF CONVERGENCE BEHAVIOR

In order to demonstrate the efficiency of the algorithm, we choose a typical one-dimensional test system consisting of the excitation from the ground state to the first excited state ($v=0\rightarrow v=1$) in a Morse potential of the O–H bond. Although this is a simple case, we believe the conclusions regarding convergence behavior are generic. In the following calculation, all the parameters are expressed in atomic units (a.u.). The Morse potential[10]

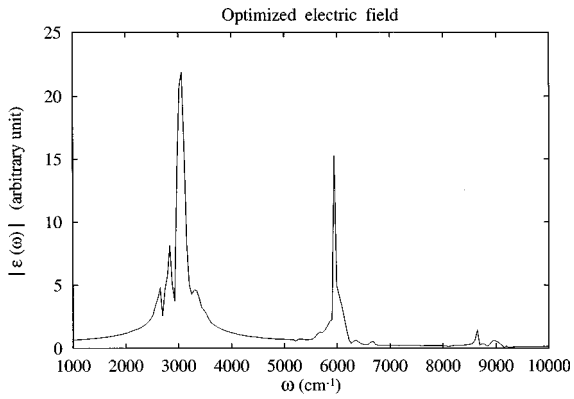


FIG. 8. Power spectrum of the field in Fig. 7. The dominant frequency matches the resonant condition of $4\rightarrow 5$. The remaining structure is identified in Table I.

TABLE I. Spectral feature assignment in Fig. 9.

| Optimal peaks[a] | Resonance energies | Assignments[b] |
|---|---|---|
| (s) 3064 $cm^{-1}$ | 3057 $cm^{-1}$ | (**4**) → (**5**) |
| (s) 5947 $cm^{-1}$ | 5937 $cm^{-1}$ | (**4**) → (**6**) |
| (s) 2836 $cm^{-1}$ | 2879 $cm^{-1}$ | (**5**) ← (**6**) |
| (w) 8645 $cm^{-1}$ | 8637 $cm^{-1}$ | (**4**) → (**7**) |
| (m) 2653 $cm^{-1}$ | 2701 $cm^{-1}$ | (**6**) ← (**7**) |
| (m) 3294 $cm^{-1}$ | 3236 $cm^{-1}$ | (**3**) ← (**4**) |
| (w) 6358 $cm^{-1}$ | 6293 $cm^{-1}$ | (**3**) → (**5**) |

[a]Labels (s), (m), and (w) mean strong, medium, and weak intensities, respectively.
[b](**v**) denotes the vibrational level $v$.

$$V(r)=D_0[e^{-\beta(r-r_0)}-1]^2-D_0 \tag{52}$$

has the parameters $D_0=0.1994$, $\beta=1.189$, and $\tau_0=1.821$, and the dipole moment function is taken as[11]

$$\mu(r)=\mu_0 r e^{-r/r^*}, \tag{53}$$

where $\mu_0=3.088$ and $r^*=0.6$. The initial wave function $\varphi_i(0)$ is chosen to be the Morse ground state, and the target wave function is chosen to be the Morse first excited state[12] at the final time $T=30\,000$ a.u.($\sim$0.725 ps). The trial input field is taken as $\overline{\epsilon(t)}=0$ and the penalty factor is $\alpha_0=1$.

Figure 1 shows the convergence behavior of the objective functional as well as the optimized probability versus the number of iteration steps, where the symbol $\infty$ stands for sufficient iteration steps for convergence (e.g., the relative deviation of the optimal objective functional between iteration steps 50 and 51 is less than 0.002% calculated by the new algorithms). In Fig. 1 we see that convergence of the algorithm is very fast. After only three iteration steps, the optimized objective functional is more than 80% of its maximum value. The numerical calculation verifies the prediction from Eq. (35) that additional iteration steps monotonically improve the previous iteration step by adding a positive term, and the first few steps give the major contribution corresponding to rapid convergence behavior. The convergence behavior of the transition probability is even more dramatic. It reaches $\sim$99% of its final value in only one iteration step. The converged optimized electric field shown in Fig. 2 is similar to a cosine function in the time domain. The corresponding frequency distribution in Fig. 3 displays a peak around 3770 $cm^{-1}$ which matches the resonant frequency between the ground and the first excited states of the stretch mode of the O–H bond. Experimentally it is only possible to switch-on and switch-off the fields at a finite rate, and asymptotically the field must be zero. This criterion was not rigidly enforced in the present work, but such an additional cost can be included. In the cases of this paper, the optimal electric fields contain many oscillations and the switch-on and switch-off effects should be insignificant.

Since only the probability is under control, in Fig. 4 we display the results of the square modulus of the final wave function and $\phi_f$ for comparison. They agree extremely well, but the slight difference is real as explained in the analysis of Eqs. (17)–(20). Actually, not only at the final time, but also at any time from 0 to $T$, the moduli of the functions $\psi_f(t)$ and $\psi_i(t)$ follow each other very well. This observation may be useful for developing additional control algorithms.

In order to show the efficiency of the algorithm, a comparison is also made with the conjugate gradient method in Fig. 5. The figure shows that the conjugate gradient method also takes a few steps to converge to high accuracy (note that

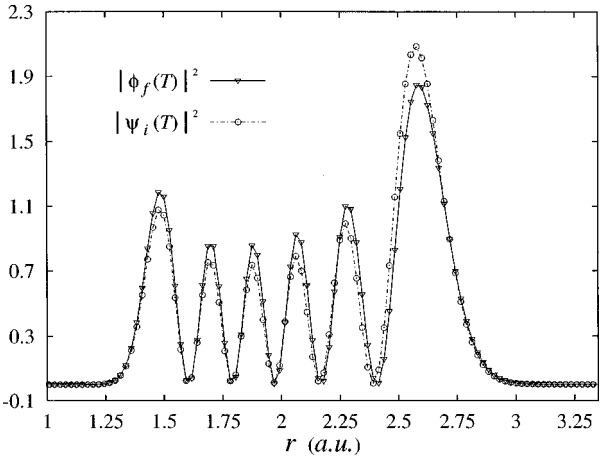


FIG. 9. Specified final wave function $|\phi_f(T)|^2$ of $v=5$ and the optimized wave function from $v=4$ at the final time $|\psi_i(T)|^2$.

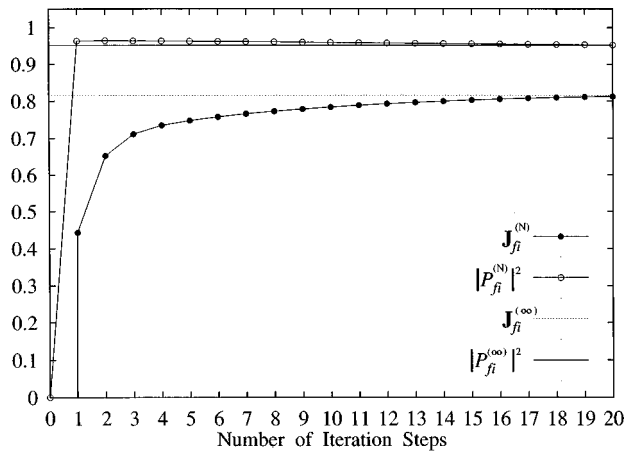


FIG. 10. Optimized objective functional $\mathbf{J}_{fi}^{(N)}$ and transition probability $|P_{fi}^{(N)}|^2$ for the transition of $v=3\rightarrow v=5$. Rapid monotonic convergence is found.

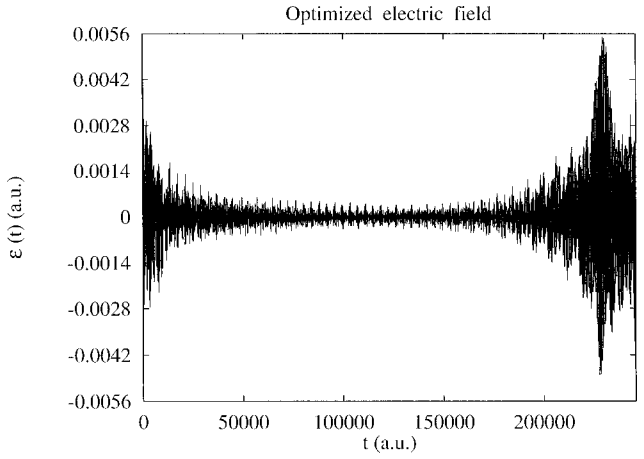


FIG. 11. Optimized electric field time dependence for the transition of $v=3\rightarrow v=5$.

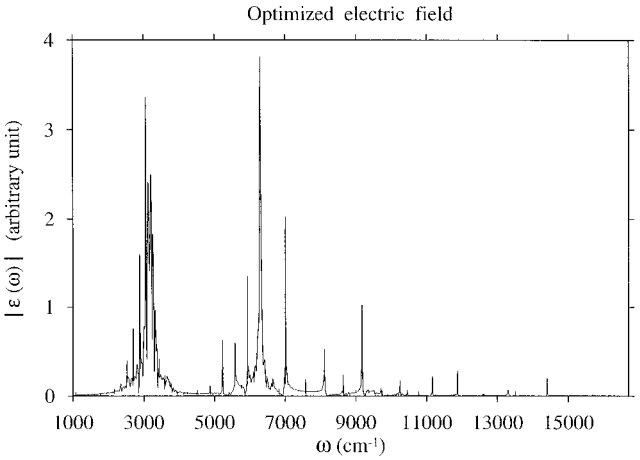


FIG. 12. Power spectrum of the field in Fig. 11. The dominant frequency matches the overtone resonant condition of $3\rightarrow 5$ and the other main pathways are $3\rightarrow 4\rightarrow 5$ and $3\rightarrow 6\rightarrow 5$. The remaining other features are identified in Table II as several additional pathways to the target $v=5$ state.

one step of the conjugate gradient method is operationally equivalent to several steps of the present algorithm). However, this result is misleading as here the initial guess of $\overline{\epsilon(t)}=0$ happens to be a good reference point to start the iteration. If we employ, for example, the guess of $\overline{\epsilon(t)}=0.5$, the convergence behavior for the present algorithm remains almost unchanged, while the conjugate gradient method needs additional iteration steps to achieve convergence. If the initial field guess is even further removed from the optimal solution, then the present algorithm was always found to be convergent almost independent of the initial guess, while the conjugate gradient method did not converge for a bad guess. We should emphasize here that neither the gradient methods nor the new algorithms are guaranteed to achieve the global minimum. Whether a local or global minimum is achieved depends on the variational functional and the algorithm employed for minimizing the variational functional. We found that the optimal electric fields calculated by the gradient methods and by the new algorithms agree very well if they achieve the same minimum point of the variational functional by proper initial guesses. As pointed out earlier, the algorithm illustrated here is only one of a family of related algorithms. The algorithm in the Appendix was even somewhat more rapidly convergent as might be expected from a comparison of Eqs. (35) and (A20).

The following example is control of the vibrational transition $v=4\rightarrow v=5$. Figure 6 shows the convergence behavior. The objective functional in the beginning has a large negative value since the initial guess of the field is far removed from the optimal solution (in this case the gradient method usually does not converge). After three iteration steps, the objective functional is more than 80% of its maximum value. Figure 7 is the optimal solution for the electric field which is more complicated than the case in Fig. 2.

TABLE II. Spectral feature assignment in Fig. 12.

| Optimal peaks[a] | Resonance energies | Assignments[b] |
|---|---|---|
| (s) 6296 $cm^{-1}$ | 6293 $cm^{-1}$ | (**3**) → (**5**) |
| (s) 3249 $cm^{-1}$ | 3236 $cm^{-1}$ | (**3**) → (**4**) |
| (s) 3058 $cm^{-1}$ | 3057 $cm^{-1}$ | (**4**) → (**5**) |
| (s) 5937 $cm^{-1}$ | 5936 $cm^{-1}$ | (**4**) → (**6**) |
| (m) 8638 $cm^{-1}$ | 8637 $cm^{-1}$ | (**4**) → (**7**) |
| (m) 11 161 $cm^{-1}$ | 11 160 $cm^{-1}$ | (**4**) → (**8**) |
| (s) 9174 $cm^{-1}$ | 9172 $cm^{-1}$ | (**3**) → (**6**) |
| (s) 2884 $cm^{-1}$ | 2879 $cm^{-1}$ | (**5**) ← (**6**) |
| (m) 11 879 $cm^{-1}$ | 11 873 $cm^{-1}$ | (**3**) → (**7**) |
| (m) 2699 $cm^{-1}$ | 2701 $cm^{-1}$ | (**6**) ← (**7**) |
| (m) 5577 $cm^{-1}$ | 5580 $cm^{-1}$ | (**5**) ← (**7**) |
| (w) 14 398 $cm^{-1}$ | 14 396 $cm^{-1}$ | (**3**) → (**8**) |
| (m) 2525 $cm^{-1}$ | 2523 $cm^{-1}$ | (**7**) ← (**8**) |
| (m) 5224 $cm^{-1}$ | 5224 $cm^{-1}$ | (**6**) ← (**8**) |
| (m) 8108 $cm^{-1}$ | 8103 $cm^{-1}$ | (**5**) → (**8**) |
| (s) 7008 $cm^{-1}$ | 7006 $cm^{-1}$ | (**1**) ← (**3**) |
| (w) 13 304 $cm^{-1}$ | 13 299 $cm^{-1}$ | (**1**) → (**5**) |

[a]Labels (s), (m), and (w) mean strong, medium, and weak intensities, respectively.
[b](**v**) denotes the vibrational level $v$.

Figure 8 shows the power spectrum and by comparison to the vibrational energy levels we can assign the peaks as indicated in Table I. The assignment shows that the optimal electric field involves not only the direct pathway $4\rightarrow 5$ but also some Raman-like indirect routes dominated by $4\rightarrow 6\rightarrow 5$. In Fig. 9, we see that the wave function at the final time, which is guided by the optimal field from the initial eigenstate of $v=4$, roughly matches the eigenstate of $v=5$.

In a further example, we optimized the transition $v=3\rightarrow v=5$. Figure 10 shows the convergence of the objective functional in which the maximum value is a little less than that in the transition of $4\rightarrow 5$ apparently because the transition $3\rightarrow 5$ requires more energy. However, as shown in Fig. 11 we allowed the total propagation time $T$ to be much larger in this case to better optimize the interference pathways induced by the electric field. The power spectrum is shown in Fig. 12, and almost all the peaks can be assigned resonant transitions as indicated in Table II. Similarly, under the control of the optimal field, propagating from the initial eigenstate of $v=3$, the wave function at the final time roughly matches the eigenstate of $v=5$, which is very similar to Fig. 9. We see that the intensity of the one-photon transition peak, $3\rightarrow 5$, is somewhat larger than that of the two-photon transition peaks, $3\rightarrow 4\rightarrow 5$. Many processes contribute to achieve the extremum value of the objective functional. The optimal solution involves a distribution of pathways which is not intuitively obvious.

More calculations show that these new methods always converge rapidly with respect to the number of iteration steps. The proper value of $T$ which captures the physical processes depends on the particular problem; this issue is inherent with control and not an algorithmic matter.

## VI. SUMMARY

In this paper, we propose a new family of effective iteration methods to solve quantum optimal control problems. The analysis shows that they are monotonically and quadratically convergent. In the first few iteration steps, usually about three, the new methods were found to converge to more than 80% of their final value almost independent of the initial guess for the control field. The present new methods are also promising for efficiently solving more general quantum optimal control problems.

## APPENDIX

The text presented one member of a family of iteration algorithms based on the interpretive use of Eq. (5) for solving Eqs. (7) and (8). Here we further illustrate the flexibility involved by summarizing another choice based on Eq. (5) which has very attractive convergence properties. This new algorithm is defined as

Step 1:

$$i\frac{\partial}{\partial t}\psi_f^{(0)}(t)=(H_0+V)\psi_f^{(0)}(t)-\mu\overline{\epsilon(t)}\psi_f^{(0)}(t), \tag{A1}$$

$$i\frac{\partial}{\partial t}\psi_i^{(1)}(t)=(H_0+V)\psi_i^{(1)}(t)+\frac{\mu}{\alpha_0}\psi_i^{(1)}(t)\times \mathrm{Im}(\langle\varphi_i(0)|\psi_f^{(0)}(0)\rangle\langle\psi_f^{(0)}(t)|\mu|\psi_i^{(1)}(t)\rangle). \tag{A2}$$

Step 2:

$$i\frac{\partial}{\partial t}\psi_f^{(1)}(t)=(H_0+V)\psi_f^{(1)}(t)+\frac{\mu}{\alpha_0}\psi_f^{(1)}(t)\times \mathrm{Im}(\langle\psi_i^{(1)}(T)|\phi_f(T)\rangle\langle\psi_f^{(1)}(t)|\mu|\psi_i^{(1)}(t)\rangle), \tag{A3}$$

$$i\frac{\partial}{\partial t}\psi_i^{(2)}(t)=(H_0+V)\psi_i^{(2)}(t)+\frac{\mu}{\alpha_0}\psi_i^{(2)}(t)\times \mathrm{Im}(\langle\varphi_i(0)|\psi_f^{(1)}(0)\rangle\langle\psi_f^{(1)}(t)|\mu|\psi_i^{(2)}(t)\rangle), \tag{A4}$$

$$\vdots$$

in which the corresponding control field at each iteration step can be written as

$$\overline{\epsilon(t)}=0(\text{or another chosen function}),$$

$$\alpha_0\epsilon^{(0)}(t)=-\mathrm{Im}(\langle\varphi_i(0)|\psi_f^{(0)}(0)\rangle\langle\psi_f^{(0)}(t)|\mu|\psi_i^{(1)}(t)\rangle), \tag{A5}$$

$$\alpha_0\epsilon^{(1)}(t)=-\mathrm{Im}(\langle\psi_i^{(1)}(T)|\phi_f(T)\rangle\langle\psi_f^{(1)}(t)|\mu|\psi_i^{(1)}(t)\rangle), \tag{A6}$$

$$\alpha_0\epsilon^{(2)}(t)=-\mathrm{Im}(\langle\varphi_i(0)|\psi_f^{(1)}(0)\rangle\langle\psi_f^{(1)}(t)|\mu|\psi_i^{(2)}(t)\rangle), \tag{A7}$$

$$\vdots$$

We see that the difference between this algorithm and the one in the text resides in the evaluation of the term, $\langle\psi_i(T)|\phi_f(T)\rangle$. If the wave functions $\psi_i^{(n)}(t)$ and $\psi_f^{(n)}(t)$ are exact, then different choices for $\langle\psi_i(T)|\phi_f(T)\rangle$, either $\langle\psi_i(t)|\psi_f(t)\rangle$ or $\langle\varphi_i(0)|\psi_f(0)\rangle$, are equivalent according to Eq. (6). However, during the iteration, they can be different because usually Eq. (6) is not exactly satisfied. Different choices for $\langle\psi_i(T)|\phi_f(T)\rangle$ can result in different convergence behavior. In the algorithm of Eqs. (9)–(15), we chose the continuous form, $\langle\psi_i^{(n)}(t)|\psi_f^{(n)}(t)\rangle$. In the algorithm of Eqs. (A1)–(A7), we chose the two-point forms, $\langle\psi_i^{(n)}(T)|\phi_f(T)\rangle$ and $\langle\varphi_i(0)|\psi_f^{(n)}(0)\rangle$.

After the first iteration step, Eqs. (A1) and (A2), we have

$$\alpha_0\epsilon^{(0)}(t) = -\mathrm{Im}(\langle\psi_f^{(0)}(t)|\mu|\psi_i^{(1)}(t)\rangle\langle\varphi_i(0)|\psi_f^{(0)}\rangle)$$
$$= -\mathrm{Im}\left(\frac{-i}{\epsilon^{(0)}(t)-\overline{\epsilon(t)}}\frac{\partial\langle\psi_f^{(0)}(t)|\psi_i^{(1)}(t)\rangle}{\partial t}\times\langle\varphi_i(0)|\psi_f^{(0)}(0)\rangle\right)$$
$$= \frac{1}{\epsilon^{(0)}(t)-\overline{\epsilon(t)}}\times\frac{\partial\,\mathrm{Re}(\langle\psi_f^{(0)}(t)|\psi_i^{(1)}(t)\rangle\langle\varphi_i(0)|\psi_f^{(0)}(0)\rangle)}{\partial t}, \tag{A8}$$

which can be equivalently changed into

$$\frac{\partial\,\mathrm{Re}(\langle\psi_f^{(0)}(t)|\psi_i^{(1)}(t)\rangle\langle\varphi_i(0)|\psi_f^{(0)}(0)\rangle)}{\partial t} = \alpha_0\epsilon^{(0)}(t)[\epsilon^{(0)}(t)-\overline{\epsilon(t)}]. \tag{A9}$$

After integration over $t$ from 0 to $T$, we will get

$$\mathrm{Re}(\langle\phi_f(T)|\psi_i^{(1)}(T)\rangle\langle\varphi_i(0)|\psi_f^{(0)}(0)\rangle) = |\langle\psi_f^{(0)}(0)|\varphi_i(0)\rangle|^2+\alpha_0\int_0^T\epsilon^{(0)}(t)[\epsilon^{(0)}(t)-\overline{\epsilon(t)}]dt. \tag{A10}$$

We can further transform it into the expression

$$|\langle\phi_f(T)|\psi_i^{(1)}(T)\rangle|^2 = |\langle\psi_f^{(0)}(0)|\varphi_i(0)\rangle|^2+2\alpha_0\int_0^T\epsilon^{(0)}(t)[\epsilon^{(0)}(t)-\overline{\epsilon(t)}]dt + |\langle\phi_f(T)|\psi_i^{(1)}(T)\rangle-\langle\psi_f^{(0)}(0)|\varphi_i(0)\rangle|^2, \tag{A11}$$

which is just the first iteration step optimized transition probability. Straightforwardly, we can deduce the expression for the first iteration step optimized objective functional:

$$\mathbf{J}_{fi}^{(0)} = |\langle\psi_f^{(0)}(0)|\varphi_i(0)\rangle|^2+2\alpha_0\int_0^T\epsilon^{(0)}(t)[\epsilon^{(0)}(t)-\overline{\epsilon(t)}]\times dt-\alpha_0\int_0^T[\epsilon^{(0)}(t)]^2dt+|\langle\phi_f(T)|\psi_i^{(1)}(T)\rangle - \langle\psi_f^{(0)}(0)|\varphi_i(0)\rangle|^2. \tag{A12}$$

Similarly, after finishing the second iteration step in Eqs. (A3) and (A4), we will obtain

$$|\langle\psi_f^{(1)}(0)|\varphi_i(0)\rangle|^2 = |\langle\phi_f(T)|\psi_i^{(1)}(T)\rangle|^2+2\alpha_0\int_0^T\epsilon^{(1)}(t)\times[\epsilon^{(1)}(t)-\epsilon^{(0)}(t)]dt+|\langle\psi_f^{(1)}(0)\times|\varphi_i(0)\rangle-\langle\phi_f(T)|\psi_i^{(1)}(T)\rangle|^2 \tag{A13}$$

and the expression for the corresponding optimized transition probability:

$$|\langle\phi_f(T)|\psi_i^{(2)}(T)\rangle|^2 = |\langle\psi_f^{(1)}(0)|\varphi_i(0)\rangle|^2+2\alpha_0\times\int_0^T\epsilon^{(2)}(t)[\epsilon^{(2)}(t)-\epsilon^{(1)}(t)]dt+|\langle\phi_f(T)|\psi_i^{(2)}(T)\rangle - \langle\psi_f^{(1)}(0)|\varphi_i(0)\rangle|^2. \tag{A14}$$

The associated optimized objective functional is

$$\mathbf{J}_{fi}^{(1)} = |\langle\phi_f(T)|\psi_i^{(2)}(T)\rangle|^2-\alpha_0\int_0^T[\epsilon^{(2)}(t)]^2. \tag{A15}$$

Following the same procedure, after the $(N+1)$th iteration step, the optimized transition probability is evaluated by

$$|P_{fi}^{(N)}|^2 = |\langle\phi_f(T)|\psi_i^{(N+1)}(T)\rangle|^2. \tag{A16}$$

Denoting $|S_{fi}^{(N)}|^2$, $\delta P_{k+1}$, and $\delta S_{k+2}$ as

$$|S_{fi}^{(N)}|^2 = |\langle\psi_f^{(N)}(0)|\varphi_i(0)\rangle|^2, \tag{A17}$$
$$\delta P_{k+1} = P_{fi}^{(k+1)}-S_{fi}^{(k+1)}, \quad k=0,1,..., \tag{A18}$$
$$\delta S_{k+2} = S_{fi}^{(k+2)}-P_{fi}^{(k+1)}, \quad k=0,1,..., \tag{A19}$$

we can obtain a simple result for the deviation of the objective functionals:

$$\delta\mathbf{J}_{NO} = \alpha_0\int_0^T\sum_{k=0}^{2N-1}|\delta\epsilon_{k+1,k}|^2dt+\sum_{k=0}^{N-1}|\delta P_{k+1}|^2+\sum_{k=0}^{N-2}|\delta S_{k+2}|^2, \tag{A20}$$

where the definitions of $\delta\epsilon_{k+1,k}$ and $\delta\mathbf{J}_{N0}$ appeared previously.

We see that the new algorithm above also has a variational character. Furthermore, comparing to the result of the algorithm in Eq. (35), we see that the algorithm here is expected to generally converge faster due to the additional positive term in Eq. (A20). Note that the numerical value of $\delta\epsilon_{k+1,k}$ in Eqs. (35) and (A20) will generally differ so that an absolute comparison of the convergence rates is application dependent. Nevertheless it was found that the algorithm in the Appendix converged more rapidly with the same numerical example employed in Fig. 1.

## ACKNOWLEDGMENTS

The authors acknowledge support from the National Science Foundation and the Office of Naval Research. W. Z. thanks Dr. Xuguang Hu and Dr. Genyuan Li for helpful discussions.

[1] A. P. Pierce, M. A. Dahleh, and H. Rabitz, Phys. Rev. A **37**, 4950 (1988).
[2] S. Shi and H. Rabitz, J. Chem. Phys. **92**, 364 (1992).
[3] M. Demiralp and H. Rabitz, Phys. Rev. A **47**, 830 (1993).
[4] D. J. Tannor, V. A. Kazakov, and V. Orlov, in *Time-Dependent Quantum Molecular Dynamics*, edited by J. Broeckhove and L. Lathouwers (Plenum, New York, 1992).

[5] J. Somloi, V. A. Kazakov, and D. J. Tannor, Chem. Phys. **172**, 85 (1993).
[6] S. Shi, A. Woody, and H. Rabitz, J. Chem. Phys. **88**, 6870 (1988).
[7] S. Shi and H. Rabitz, Comput. Phys. Commun. **63**, 71 (1991).
[8] W. Jakubetz, B. Just, J. Manz, and H. Schreier, J. Phys. Chem. **94**, 294 (1990).
[9] J. E. Combariza, B. Just, J. Manz, and G. K. Paramonov, J. Phys. Chem. **95**, 10351 (1991).
[10] G. K. Paramonov, Chem. Phys. **177**, 169 (1993).
[11] R. T. Lawton and M. S. Child, Mol. Phys. **40**, 773 (1980).
[12] M. L. Sage, Chem. Phys. **35**, 375 (1978).